Vol.1, Issue 2, June 2026.

CENTRAL ASIAN TRANSACTIONS ON MATERIALS STRUCTURE AND PROPERTIES

https://doi.org/10.51885/3134-7983_CATMSP_2026_2_2
SRSTI 53.37.13

INVESTIGATION INTO THE LEACHING KINETICS AND MECHANISM OF NICKEL EXTRACTION FROM ASBESTOS TAILINGS VIA NITRIC ACID TREATMENT

Omirserik Baigenzhenov [1]*, Assel Dagubayeva [2], Galymzhan Maldybayev [2], Rustam Sharipov [2], Aliya Alimzhanova [3]

[1]Satbayev University, Almaty, Kazakhstan
[2]Kazakh-British Technical University, Almaty, Kazakhstan
[3]National Center for Complex Processing of Mineral Raw Materials of the Republic of Kazakhstan, Almaty, Kazakhstan
*Corresponding author: Baigenzhenov Omirserik, o.baigenzhenov@satbayev.university

keywords:
Asbestos waste, magnetic fraction, nickel, nitric acid leaching, kinetic modeling, activation energy.

ABSTRACT

This study presents the results of an investigation into the kinetics of nitric acid leaching of nickel from the magnetic fraction of chrysotile asbestos beneficiation waste. The relevance of this work stems from the necessity to involve large-tonnage technogenic formations into processing circuits. It was established that the application of magnetic separation enables preliminary concentration of nickel, thereby enhancing the efficiency of subsequent hydrometallurgical processing. The experimental study examined the influence of temperature (25–85 °C) and process duration on the extraction degree of the valuable component. To identify the reaction mechanism, kinetic modeling was performed using the Jander, Drozdov-Rotinyan, Prout-Tompkins, and Johnson-Mehl-Avrami-Kolmogorov (JMAK) equations. The calculated apparent activation energy (E_a = 18.4 kJ mol^{-1}) indicates that the process proceeds under diffusion-controlled conditions. The obtained results establish a scientific and practical foundation for developing a low-waste technology for processing asbestos tailings with the concurrent production of marketable nickel compounds.

INTRODUCTION

At the current stage of development in the mining and metallurgical industry, the processing of anthropogenic waste has become a strategically vital area that aligns environmental safety principles with economic efficiency within the circular economy framework. In Kazakhstan, over 300 million tons of serpentinite waste have accumulated as a result of long-term chrysotile asbestos mining and beneficiation (Shayakhmetova et al. 2024). These tailings not only remove significant land areas from economic use but also impose a substantial environmental burden on the region. According to technological data, during asbestos ore processing, commercial fiber accounts for only 6–8% of the total mined mass, while over 92% is classified as waste. Nevertheless, these anthropogenic deposits represent a valuable secondary resource: a nickel content of 0.2–0.4% suggests total metal reserves in the range of 600-1,200 thousand tons. Given that the raw material is already comminuted and located on the surface, its development is highly promising (Baigenzhenov et al. 2015).

The relevance of nickel extraction from such sources is dictated by its critical role in the production of stainless steels, high-temperature alloys, and, most importantly today, the energy storage sector (Abdirashit et al. 2025). Nickel is a fundamental component of cathode materials for lithium-ion batteries, the demand for which is growing exponentially. Amid the depletion of high-grade sulfide deposits, the transition to processing low-grade oxidized silicate-type resources is becoming inevitable (Tauakelov et al. 2025, Kelamanov et al. 2021). However, the effective implementation of this transition requires a profound understanding of the raw material's crystal chemistry. It is important to note that nickel in chrysotile waste is characterized by a complex distribution: approximately 65–70% of its total volume is closely associated with iron minerals, while only the remainder is involved in the isomorphic substitution of magnesium ions within the crystal lattices of lizardite, antigorite, and chrysotile. This specificity precludes the use of mechanical beneficiation methods and necessitates chemical treatment to decompose the mineral matrix.

In global and domestic practice, most existing technologies for processing serpentinite raw materials are oriented toward the use of hydrochloric or sulfuric acids. An example of the industrial application of the hydrochloric acid scheme is the Canadian Magnola technology (Chen et al. 2000), as well as numerous studies by Russian (Kovalevskiy et al. 2024) and Kazakhstani scientists (Shevko et al. 2022) aimed at producing synthetic carnallite and bischofite (Arynov et al. 2017). Sulfuric acid technologies, in turn, are traditionally aimed at the production of magnesium sulfate salts. Despite the availability of established schemes for these reagents, the use of nitric acid (HNO_3) in this context remains significantly under-researched. Meanwhile, nitric acid technology possesses substantial potential due to the high reactivity of the reagent, the possibility of nearly complete acid regeneration, and the production of valuable nitrate products, which aligns with the principles of «green» metallurgy. However, these conventional schemes exhibit significant operational limitations that hinder their sustainable application to low-grade silicate wastes. Hydrochloric acid leaching is constrained by high reagent volatility, toxic fuming, and aggressive chloride-induced pitting corrosion, which necessitates the use of expensive acid-resistant alloys (e.g., Hastelloy, titanium) and complex off-gas scrubbing systems. Sulfuric acid processing, although widely implemented, inevitably leads to gypsum ($CaSO_4 \cdot 2H_2O$) precipitation even at low calcium concentrations; this increases pulp viscosity and complicates downstream solid–liquid separation. In contrast, nitric acid offers distinct technological advantages: its strong oxidative potential facilitates the decomposition of refractory Fe–Ni spinels, it forms highly soluble nickel nitrate complexes that prevent passivating scale formation, and it exhibits significantly lower corrosivity toward passivated stainless steel alloys compared to chloride-based media. Moreover, established denitration and absorption technologies enable efficient recovery and regeneration of HNO_3 from pregnant leach solutions, substantially reducing reagent consumption and aligning the process with circular economy principles.

The lack of systemic literature data on the interaction mechanisms between nickel compounds and nitric acid creates a serious gap that hinders the industrial implementation of this method. Understanding the process kinetics is a fundamental requirement for identifying the rate-limiting step of the interaction - whether it be the chemical reaction itself or the diffusion of reagents through the resulting solid product layer [Baigenzhenov et al. 2024, Ivanov et al. 2025]. Without establishing precise mathematical dependencies of the nickel extraction rate on temperature, acid concentration, and stirring intensity, it is impossible to scale up laboratory data to the level of industrial equipment.

Despite the theoretical benefits of the nitric acid route, systematic kinetic data for complex anthropogenic silicate matrices remain absent in the literature. The scientific novelty of this study lies in the first comprehensive evaluation of the magnetic fraction of chrysotile

asbestos beneficiation tailings as a dedicated secondary nickel resource. Accounting for an accumulated waste volume of approximately 350 million tons with an average NiO content of 0.25 wt.%, the recoverable nickel reserve exceeds 875 thousand tons, representing a strategically significant, pre-comminuted, and surface-accessible feedstock. Furthermore, this work provides the first rigorous kinetic modeling of nitric acid leaching applied to this specific feedstock, establishing an apparent activation energy of 18.4 kJ/mol and conclusively identifying internal diffusion through the porous reaction product layer as the rate-limiting step.

Based on the above, the objective of the present work is to study the kinetic patterns of the nitric acid leaching of nickel from anthropogenic asbestos production waste. During the study, the applicability of modern kinetic models to describe the process was evaluated, and key parameters such as activation energy and rate constants were determined. The results are intended to form a science-based foundation for developing an innovative technology for the complex processing of secondary nickel-containing raw materials, thereby expanding the resource base of this strategically important metal and reducing the environmental burden in industrial regions.

MATERIALS, METHODS AND EQUIPMENT

Sampling and characterization

The raw material used for nickel extraction in this study consisted of asbestos production waste from the Zhitikara deposit, generated during the production of asbestos fibers. Sample pretreatment included grinding the material in a ball mill, followed by sieve analysis to isolate the fraction with a particle size of less than 0.25 mm. The resulting fine fraction was subjected to dry magnetic separation at a magnetic field strength of 1500 Oersteds. As a result of the separation, a magnetic fraction was isolated with a yield of 5.0–5.5% of the initial mass. The nickel concentration in the pregnant leach solutions was measured using a Shimadzu AA-7000 series atomic absorption spectrometer (AAS) in air–acetylene flame mode. The wavelength for nickel detection was 232.0 nm, with a spectral slit width of 0.2 nm. The calibration curve was constructed using standard solutions in the concentration range of 0.5–5.0 mg·L^{-1}. For each sample, measurements were performed in triplicate, and the relative standard deviation (RSD) did not exceed 3%, confirming acceptable precision under the adopted experimental conditions.

The phase composition and identification of mineral forms were performed using X-ray diffraction (XRD). Diffraction patterns were recorded on a Bruker D8 Advance X-ray diffractometer equipped with a LynxEye strip detector. Cu Kα radiation (λ = 1.5406 Å) was generated at 40 kV and 40 mA. Data were collected over a 2θ range of 10° to 80° with a step size of 0.015° and a counting time of 0.2 s per step. Phase identification was carried out using the DIFFRAC.EVA software package (Bruker AXS) in conjunction with the PDF-2 (ICDD) database. Semi-quantitative phase analysis was performed using the Rietveld refinement method implemented in the TOPAS software (Bruker AXS).

Surface morphology and local elemental composition were investigated using scanning electron microscopy combined with energy-dispersive X-ray spectroscopy (SEM/EDS). A JEOL JSM-6490LV scanning electron microscope equipped with an Oxford Instruments INCA Energy 250 X-ray microanalysis system was employed. The accelerating voltage was set to 20 kV, the working distance was adjusted to 10 mm, and the beam current was kept at approximately 1 nA. The EDS spectra were acquired for 60 seconds of real accumulation time to ensure adequate signal-to-noise ratio. Semi-quantitative elemental analysis was performed using the INCA Energy software package with the ZAF (Z=Atomic number, A=Absorption, F= Fluorescence) correction procedure. The typical analytical uncertainty for semi-quantitative XRD phase analysis was estimated at ±3 wt.%, while EDS elemental quantification showed a relative error of ≤5 wt.% for major elements.

Detailed information regarding the phase composition and microstructure features is presented in Figures 1 and 2. The diffraction pattern shown in Fig. 1 identifies the complex mineralogical composition of the magnetic fraction. The predominant phases are magnetite ($Mg_{0.04}Fe_{2.96}O_4$) and antigorite ($Mg_3Si_2O_5(OH)_4$) confirmed by characteristic reflections in the 2θ region. The presence of lizardite ($Mg_3Si_2O_5(OH)_4$) and nickel ferrite ($NiFe_2O_4$) was also recorded, with the latter's content estimated at approximately 3.3% according to semi-quantitative analysis. The presence of ferrite phases explains the magnetic properties of the concentrate and indicates that a significant portion of the nickel is associated with iron-bearing mineral forms.

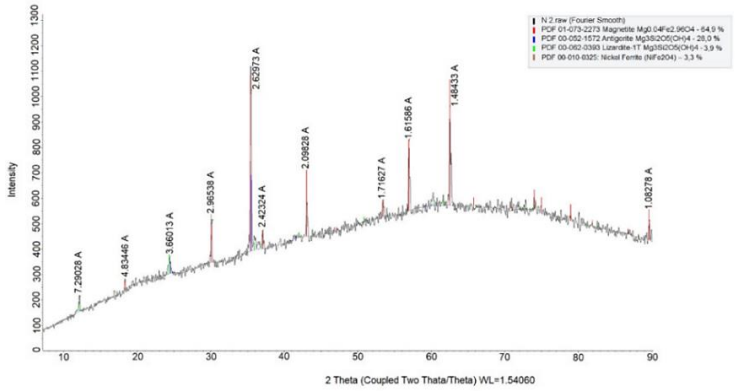

Figure 1. The XRD pattern of the magnetic fraction

Note – compiled by the authors

The surface micromorphology of the magnetic fraction is characterized by particles of irregular, angular shapes with pronounced size heterogeneity (Figure 1). The energy-dispersive spectrum (EDS) confirms the complex elemental profile of the material. According to the local microanalysis results, the primary components are nickel (47.18 wt.%), iron (21.96 wt.%), and magnesium (7.94 wt.%). The high nickel concentration at the analyzed point confirms the effectiveness of the preliminary magnetic beneficiation and the feasibility of utilizing this raw material for subsequent hydrometallurgical processing. The presence of silicon and oxygen correlates with the XRD data regarding the occurrence of silicate and oxide mineral phases.

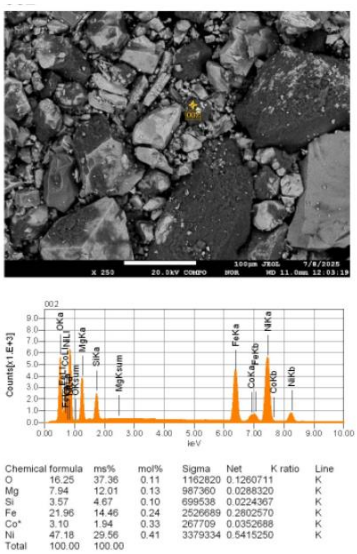

Figure 2. SEM micrograph and corresponding EDS spectrum of the magnetic fraction

Note – compiled by the authors

Leaching Procedure

Leaching experiments were conducted in batch mode using a sealed glass flask. A 25.0 g sample of the magnetic fraction was placed into the reactor, which was sealed with a two-neck rubber stopper: one neck was used for the shaft of an overhead stirrer with an impeller, while the second served for liquid phase sampling. To maintain a stable temperature throughout the experiment, a thermostatic water bath with a regulation accuracy of ±1 °C was employed. To prevent temperature fluctuations at the onset of the reaction, both the solid sample and the nitric acid solution were pre-thermostated to the target temperature. The process commenced upon the introduction of the heated solvent into the reactor containing the solid sample, simultaneous with the activation of the stirring system. The nitric acid concentration of 25 wt.% (~4.0 M) was selected based on stoichiometric estimation. For a 25.0 g sample of the magnetic fraction (containing ~2.2 wt.% NiO, ~22 wt.% Fe, and ~8 wt.% Mg), theoretical calculations indicated a minimum HNO_3 requirement of ~0.27 mol to dissolve the target metal oxides. Aliquots were sampled at specified time intervals of 30, 60, 90, 120, 150, and 180 minutes. At each stage, a 5.0 mL filtrate sample was collected, quantitatively transferred to a volumetric flask, and diluted to 250 mL with deionized water. The concentrations of nickel and cobalt in the resulting solutions were determined via atomic absorption spectrometry (AAS). To ensure the reliability of the results and assess reproducibility, all experiments were performed in triplicate, with subsequent calculation of the mean values. Statistical analysis of the replicate measurements showed that the relative standard deviation (RSD) for all leaching efficiency data did not exceed 5%, confirming acceptable precision and reproducibility of the experimental results. Prior to each experiment, all laboratory glassware was thoroughly cleaned with deionized water. The leaching efficiency (LE) for Ni was calculated as the percentage of the total nickel mass transferred into the solution relative to its initial content in the solid sample, according to the following equation:

$$LE(\%) = \frac{C_{Ni} \cdot V}{m_{sample} \cdot w_{Ni}} \cdot 100, \quad (1)$$

where: C_{Ni} (gL^{-1}) is the concentration of Ni in the leach liquor;

V (L) is the leach liquor volume;

m_{sample} – mass of the magnetic fraction sample taken for leaching (g);

w_{Ni} – is the mass fraction of Ni in the original magnetic fraction (dimensionless, e.g., 0.022 for 2.2 wt.%).

Kinetic analysis and theoretical modeling

To gain a profound understanding of the nickel extraction mechanism from the magnetic fraction of asbestos waste and to identify the rate-limiting step of the process, a kinetic analysis of the experimental data was performed. The leaching process in a solid-liquid system is multi-stage and may be controlled by the rate of chemical interaction at the phase interface, the diffusion of reagents through the boundary layer, or diffusion through the solid product layer (filter cake) (Kenzhaliyev et al. 2025).

To quantitatively evaluate the kinetic parameters and identify the rate-limiting mechanism, the experimental data were processed using a set of classical topochemical reaction models: the Jander equation (Petrovski et al. 2019), the Drozdov-Rotinyan equation (Zoraga et al. 2020), the Prout-Tompkins autocatalytic model (Zoraga et al. 2020), and the Johnson-Mehl-Avrami-Kolmogorov (JMAK) model (Fournier et al. 2018). Based on these models, the apparent activation energy of the process was calculated.

Diffusion models: Jander and Drozdov–Rotinyan equations

Given that insoluble silicate residue layers may form on the surface of magnetic particles during nitric acid leaching, hindering acid access to the reaction zone, diffusion models were considered first.

The Jander model is based on the assumption of spherical particle geometry and a parabolic law of product layer growth. This is a classical equation for systems where the diffusion of ions through a passive layer is the rate-limiting step:

$$[1 - (1 - \alpha)^{1/3}]^2 = k \cdot \tau \quad (2)$$

where: α – recovery degree, (%);

τ – is the duration of interaction, (min);

k – reaction rate constant, (is a proportionality constant for a given reaction), (min^{-1});

b – is a rate constant that describes the rate at which solutes are transferred from one medium to another.

The physical significance of this model lies in the fact that as the nickel leaching from the asbestos waste magnetic fraction progresses, an inert layer (e.g., a siliceous residue or a magnetite layer) forms at the phase interface. This layer creates a diffusion resistance that increases proportionally to the depth of conversion. A linear approximation of the experimental data in coordinates of $[1 - (1 - \alpha)^{1/3}]^2$ versus τ allows for the confirmation of the diffusion-controlled nature of the rate-limiting step.In addition to the Jander model, the Drozdov-Rotinyan model was considered, which accounts for changes in the effective phase contact surface area and is more sensitive to the porosity of the resulting solid cake. This model was developed to account for both diffusion and chemical resistance, including the deceleration of the reaction rate due to the accumulation of secondary products that may partially block the reacting surfaces or pores.

$$\frac{1}{\tau} ln\left(\frac{1}{1-a}\right) = M - \beta \frac{a}{\tau}, \quad (3)$$

where: α - recovery degree, (%);

τ- is the duration of interaction, (min);

β and M – are the coefficients of braking and total speed, respectively.

The left side of the equation incorporates both a term representing the reaction kinetics and a «retardation» term, which reflects the deceleration of the leaching process over time. This model is particularly relevant when leaching initially proceeds rapidly but subsequently slows down due to the formation of passivating layers or changes in the morphology of the solid phase.

Prout–Tompkins autocatalytic model

To describe the autocatalytic nature of nickel leaching, which is accompanied by the processes of nucleation and growth of active sites, a modified Prout–Tompkins model was utilized. In this work, the equation was applied in a linearized form that accounts for the power-law dependence of the reaction rate on time:

$$ln\left(\frac{a}{1-a}\right) = k ln\tau + b \quad (4)$$

where: α - recovery degree, (%);

k - reaction rate constant (is a proportionality constant for a given reaction), (min^{-1});

τ - is the time, (min);

b - is a rate constant that describes the rate at which solutes are transferred from one medium to another.

The choice of this equation form is necessitated by the need to account for the complex kinetics involved in the decomposition of the magnetic fraction's mineral matrix, where the formation rate of new reaction zones may vary during the interaction with the reagent.

Johnson-Mehl-Avrami-Kolmogorov (JMAK) model

For a comprehensive evaluation of the leaching mechanism, not limited to a single specific stage, the universal Johnson-Mehl-Avrami-Kolmogorov (JMAK) model was employed. This equation enables the description of heterogeneous processes occurring through the stages of nucleation and growth of a new phase and is mathematically expressed as follows:

$$ln(-ln(1 - \alpha)) = n\ ln\ \tau + lnk \quad (5)$$

where: α - recovery degree,(%);

k - reaction rate constant (is a proportionality constant for a given reaction), (min^{-1});

τ - is the time, (min);

n - the kinetic parameter (Avrami index) that determines the mechanism and the geometry of the reaction zone growth.

Determination of activation energy

In the final stage of the kinetic analysis, rate constants *(k)* are calculated for each temperature based on the most appropriate model (using the criterion of R^2=1). Using the linearized form of the Arrhenius equation, a plot of *lnk* versus *1/T* is constructed:

$$lnk = \ln A_{exp} - \frac{E_a}{RT}, \quad (6)$$

where: A_{exp} - is the frequency factor;

E_a – is the apparent activation energy, (kJ/mol);

R - is gas equilibrium constant, R = 8.314 (J/mol);

T - is the absolute temperature, (K).

The value of the apparent activation energy (Ea) serves as a decisive argument in determining the mechanism:

- E_a < 20 kJ/mol: The process is limited by external or internal diffusion. The rate is highly dependent on the stirring intensity.
- 20 < E_a < 40 kJ/mol: Mixed (intermediate) regime.
- E_a > 40 kJ/mol: Chemical control (reaction-controlled). The rate is determined by the bond-breaking energy within the mineral and is practically independent of the system's hydrodynamics (Yessengaziyev et al. 2025).

RESULTS AND DISCUSSION

The effects of leaching temperature and time

Analysis of the dependence of nickel extraction efficiency from the magnetic fraction of asbestos waste on the temperature regime and phase contact duration revealed a profound correlation between the intensity of thermal exposure and the completeness of the leaching process. The presented dependencies (Figure 3) allow for the identification of two characteristic stages of interaction within the heterogeneous «solid-liquid» system.

The first stage, covering the initial period of up to 30 minutes, is characterized by the maximum rates of the target component's transition into the solution. At a temperature of 85 °C, the extraction reaches 40.1%, which significantly exceeds the values obtained at 25 °C(12.8%). Such a correlation indicates the presence of a high energy barrier that prevents the leaching agent from freely accessing the nickel-containing phases localized deep within the mineral associations. In this context, the temperature increase acts as an activation factor, providing the necessary energy to break chemical bonds in the crystal lattice of the technogenic mineral and promoting the intensification of molecular diffusion of hydrogen ions to the reaction surface.

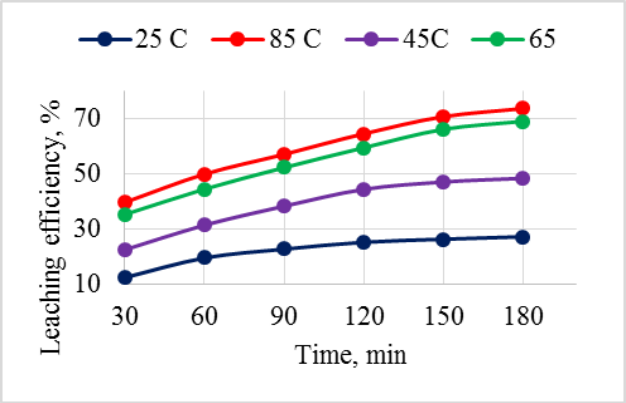

Figure 3. Effect of leaching temperature and time on the nickel recovery degree
Note – compiled by the authors

With a further increase in processing time to 180 minutes, a significant difference in the behavior of the curves is observed. Under low-temperature regimes (25 °C and 45 °C), the process demonstrates a pronounced attenuation after 60–90 minutes of the experiment, reaching a plateau at values of 27.6% and 48.8%, respectively. This phenomenon is due to the formation of a dense layer of a secondary product — an insoluble residue — around the undecomposed particles, which creates significant diffusion resistance and blocks the transport of the reagent to the active sites. In contrast, under thermal exposure of about 65–85 °C, the system maintains high reactivity throughout the entire studied interval, ensuring a final nickel yield of 69.1–74.1%.

The maintenance of a consistently high dissolution rate at elevated temperatures is explained by changes in the physicochemical properties of the boundary layer: a decrease in the dynamic viscosity of the solution and a possible change in the morphology of the resulting cake layer, which becomes more permeable to nitric acid ions. This allows for the effective refractory mineral phases, previously protected by a layer of reaction products, to be decomposed.

Visual analysis of the pregnant leach solutions obtained as a result of nitric acid leaching of the magnetic fraction confirms the significant influence of the temperature factor on the process intensity (Fig. 4).

Figure 4. Visual appearance of the solutions obtained after nitric acid leaching of the magnetic fraction at different temperatures (25°C and 85°C)
Note – compiled by the authors

The solutions obtained at temperatures of 25 °C and 85 °C are characterized by a light green coloration typical of hydrated nickel ions ($[Ni(H_2O)_6]^{2+}$). The observed qualitative similarity in the color of the solutions correlates with the quantitative analysis data, indicating nickel extraction under both temperature regimes. However, the maintained transparency of the solutions without signs of intense turbidity indicates the selectivity of the process and the absence of massive precipitation of secondary products under these conditions. This visual observation serves as additional confirmation that nickel transitions into the liquid phase in the form of stable soluble nickel (II) nitrate salts.

The effect of solid-to-liquid (S:L) ratio on nickel recovery

Based on the results obtained during the previous experiments, the optimal values for the process duration (180 min) and temperature (85 °C) were selected for further research. In this subsection, the influence of the solid-to-liquid ratio (S:L) on the nickel leaching efficiency was studied in the range from 1:2 to 1:5 (Table 1).

Table 1. Effect of solid-to-liquid (S:L) ratio on the efficiency of nickel extraction

S:L ratio	Ni leaching efficiency, %
1:2	64.7
1:3	73.8
1:4	73.8
1:5	73.8
Note – compiled by the authors	

Analysis of the obtained data shows that at an S:L ratio of 1:2, the nickel extraction was 64.7%. Such a result may be due to the high viscosity of the slurry and an insufficient volume of nitric acid solution for the complete decomposition of the mineral matrix under conditions of limited solvent volume.

When the ratio is increased to 1:3, the degree of nickel extraction rises to 73.8%. Notably, a further increase in the liquid phase volume to ratios of 1:4 and 1:5 did not lead to changes in the technological parameters: in all subsequent experiments, the extraction remained constant at 73.8%.

The stability of the results at ratios from 1:3 to 1:5 indicates that the S:L = 1:3 value is a critical point at which the optimal volume of the leaching reagent is achieved. Further dilution of the system exerts no thermodynamic or kinetic influence on the completeness of nickel transition into the solution. Thus, the S:L = 1:3 ratio was determined to be optimal, ensuring maximum extraction with efficient reagent consumption.

Kinetic modeling and mechanism identification of nickel leaching

Evaluation of diffusion limitations using the Jander model

To assess the role of internal diffusion through the product layer, the experimental data were processed using the Jander equation. The application of this model allows for determining whether the leaching rate is limited by the transport of reagents through the densifying silicate matrix formed during the decomposition of asbestos waste. As is well known, the Jander model describes the kinetics of a process controlled by internal diffusion through a forming porous product layer. The plotted graph (Figure 5) demonstrates the dependence of $[1-(1-\alpha)^{1/3}]^2$ on the leaching time at various temperatures (25, 45, 65, and 85 °C). Analysis of the coefficients of determination (R^2) shows that the degree of model fit to the experimental data increases with temperature: $R^2 = 0.8649$ at 25 °C, 0.9355 at 45 °C, 0.9798 at 65 °C, and 0.9843 at 85 °C.

The observed increase in R^2 with temperature indicates an intensification of diffusion control at elevated temperatures, which is consistent with the physicochemical characteristics of the process. At low temperatures (25 and 45 °C), the deviation from linearity may be due to

additional factors, such as the initial stage of dissolution or surface phenomena not accounted for by this model. At higher temperatures (65 and 85 °C), the predominance of diffusion control is confirmed by high R^2 values, indicating that mass transfer through the porous layer of reaction products dominates as the rate-limiting stage of the process. The slope coefficients of the lines (rate constants) increase with rising temperature, which corresponds to the acceleration of diffusion processes in accordance with the Stokes-Einstein equation (Zmpitas et al. 2021).

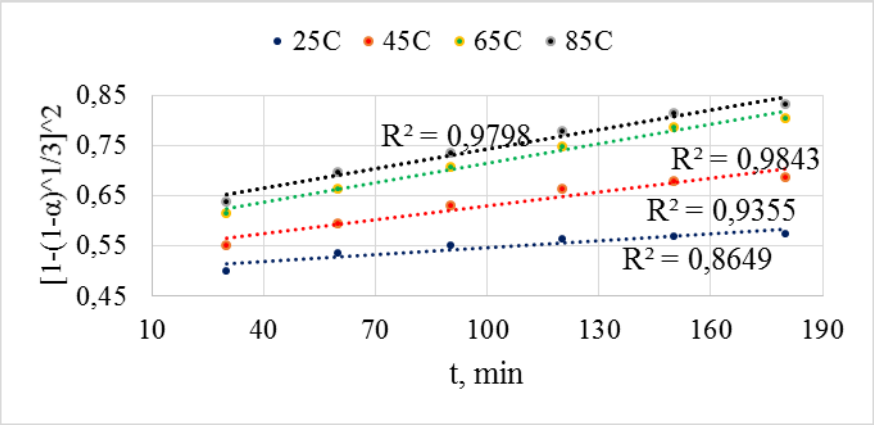

Figure 5. Linearized form of the Jander model, plotted as $[1(1\alpha)^{1/3}]^2$ versus time
Note – compiled by the authors

Assessment of the inhibition effect based on the Drozdov–Rotinyan model

The deceleration of the leaching process at later stages is often caused by the accumulation of reaction products or a reduction in the active surface area. The Drozdov - Rotinyan model was employed to quantitatively assess this inhibitory effect and to analyze the stability of the nickel extraction rate over time. The dependence of $(1/\tau)\cdot\ln[1/(1-\alpha)]$ on the α/τ ratio (Figure 6) demonstrates high linearity at all studied temperatures, with coefficients of determination R^2 = 0.9798 (25 °C), 0.9982 (45 °C), 0.9964 (65 °C), and 0.9556 (85 °C). This indicates the applicability of the Drozdov–Rotinyan model for describing the kinetics of nickel leaching.

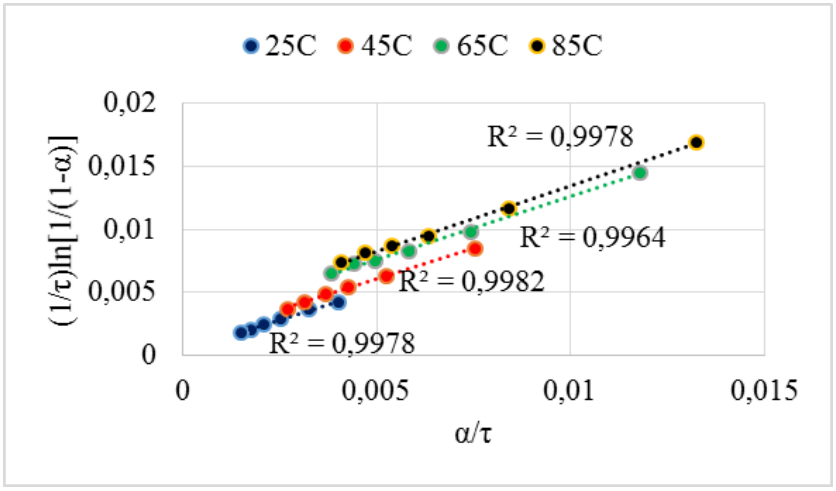

Figure 6. Linearized form of the Drozdov-Rotinyan model, plotted as $(1/\tau)\ln[1/(1-\alpha)]$ versus
Note – compiled by the authors

The Drozdov–Rotinyan model accounts for both the diffusion control and the inhibitory effect caused by the accumulation of secondary reaction products, which can block active sites or narrow the pore space (Wang et al.2025). High R^2 values confirm that the leaching process is accompanied by a significant inhibitory effect, which intensifies with an increasing degree of conversion. The negative values of the inhibition coefficient β at low temperatures indicate the absence of a pronounced passivation effect during the initial stage of the process. In contrast, with increasing temperature, the β coefficient becomes positive, which may indicate partial blocking of active sites by secondary reaction products in the later stages of leaching. A distinctive feature of this system is that the formation of a dense passivating layer does not occur, which is consistent with the morphology of the solid residue after nitric acid leaching.

Investigation of the autocatalytic nature of leaching via the Prout–Tompkins model

At the initial stages of serpentine mineral decomposition, autocatalytic behavior associated with the formation of new reaction centers may be observed. The Prout–Tompkins model was applied to test the hypothesis of process control by the nucleation and growth stage of a new phase, which is characteristic of complex transformations in «solid-liquid» systems (Doménech-Carbó. 2024). The dependence of $\ln[\alpha/(1-\alpha)]$ on the natural logarithm of time ($\ln\tau$) shown in Figure 7 demonstrates high linearity at all temperatures, with coefficients of determination R^2=0.9556 (25 °C), 0.9927 (45 °C), 0.9765 (65 °C), and 0.9784 (85 °C). The slope coefficients of the lines (parameter n) are 1.42 at 25 °C, 1.58 at 45 °C, 1.73 at 65 °C, and 1.89 at 85 °C, exceeding unity in all cases.

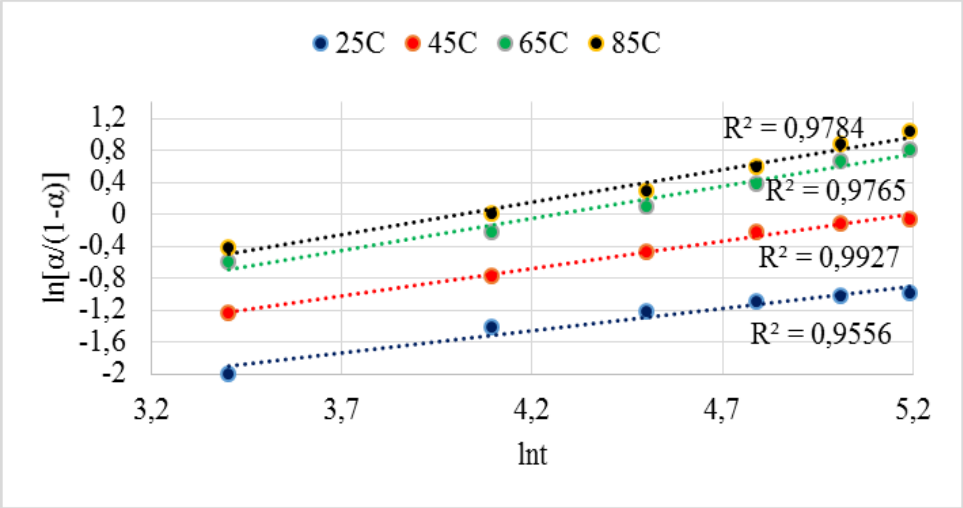

Figure 7. Linearized form of the Prout–Tompkins model, plotted as $\ln[\alpha/(1-\alpha)]$ versus $\ln\tau$

Note – compiled by the authors

Such behavior is characteristic of autocatalytic processes, where reaction products accelerate the further progress of leaching. In the nitric acid–asbestos waste system, the autocatalytic effect may be attributed to several factors:

1. the formation of soluble nickel nitrate complexes, which reduce local surface tension and improve particle wettability;
2. a local decrease in pH within the near-surface layer due to the accumulation of H^+ ions released during the hydrolysis of the silicate matrix;
3. the formation of a microporous residue structure, which increases the effective contact area between the solid and liquid phases.

The increase in the slope coefficient with temperature indicates an intensification of the autocatalytic contribution to the overall process kinetics at higher temperatures, which is consistent with accelerated ion diffusion and intensified complexation.

4.4 Determination of kinetic parameters using the JMAK model

To gain a deeper understanding of the kinetic patterns of the process, the generalized JMAK equation was used, which allows for the description of heterogeneous reactions occurring in complex solid-phase systems. This model was applied to determine the integral leaching rate constants, taking into account the cumulative influence of various physicochemical factors on nickel extraction from the magnetic fraction. The plot of $ln[-ln(1-\alpha)]$ versus $ln\tau$ demonstrates a linear behavior across the entire range of studied temperatures (Figure 8), with coefficients of determination R^2 = 0.9901 (25 °C), 0.9874 (45 °C), 0.9921 (65 °C), and 0.9911 (85 °C). The slope coefficients of the lines, corresponding to the Avrami exponent (n), vary from 0.85 at 25 °C to 1.12 at 85 °C.

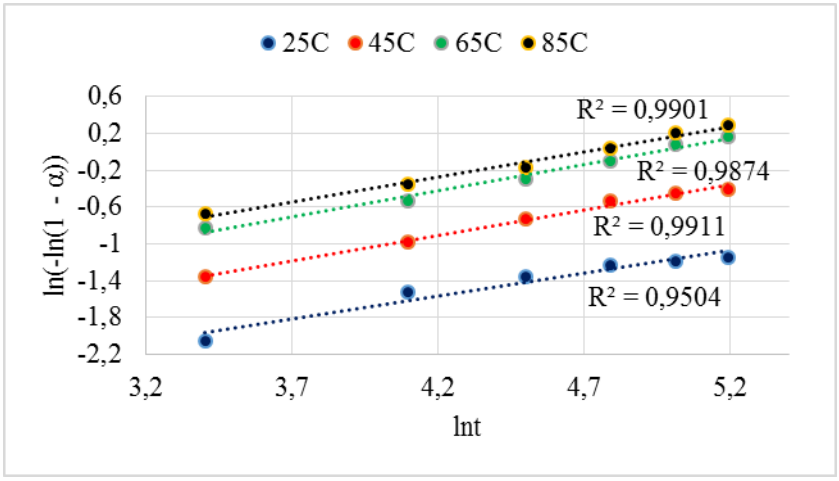

Figure 8. Linearized form of the *JMAK* model, plotted as $ln(-ln(1 - \alpha))$ versus lnτ

Note – compiled by the authors

The values of the parameter n close to unity indicate a one-dimensional growth mechanism of dissolution zones with a constant nucleation rate on the particle surfaces. A slight increase in n with temperature may suggest a transition from a predominantly surface-controlled mechanism to a combined one, incorporating elements of bulk diffusion at higher temperatures. High coefficients of determination confirm that the process of nickel leaching from the magnetic fraction of asbestos waste by nitric acid proceeds through successive stages of active dissolution center nucleation at the phase interface, followed by the radial propagation of leaching zones into the particles. This mechanism is consistent with X-ray diffraction data, which show a gradual decrease in the reflection intensity of nickel-containing spinels without the formation of new crystalline phases in the residue.

Calculation of apparent activation energy and identification of the rate-limiting step

The temperature dependence of the rate constants obtained from the previous models was analyzed using the Arrhenius law to determine the energy barrier of the process. The calculated value of the apparent activation energy allows for a definitive conclusion as to whether nickel leaching is controlled by chemical kinetics or mass transfer. The dependence of the natural logarithm of the reaction rate constant (lnk) on the reciprocal of the absolute temperature ($1000/T$) is presented in Arrhenius plots (Figure 9). The experimental points fit a straight line with a coefficient of determination R^2 = 0.968, confirming the thermally activated nature of the leaching process.

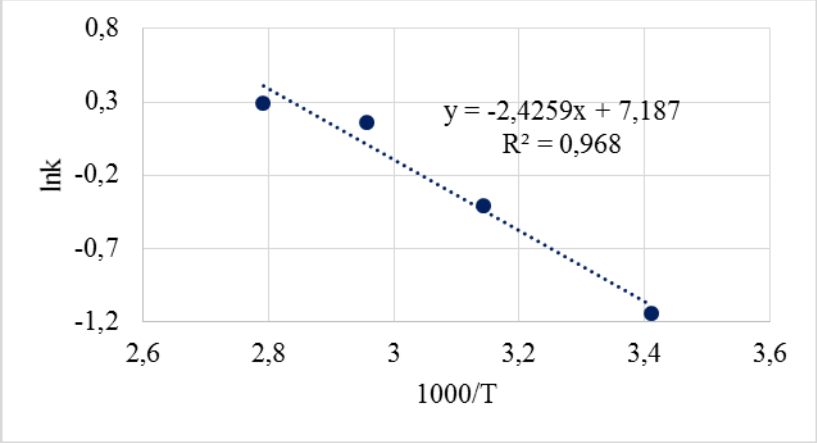

Figure 9. Arrhenius plots for the leaching of Ni

Note – compiled by the authors

Based on the slope of the resulting Arrhenius dependence, the apparent activation energy was calculated as E_a = 18.4 kJ·mol^{-1}. This value falls within the range of 10–20 kJ·mol^{-1}, which is universally recognised as characteristic of processes whose overall rate is limited by diffusion through a porous layer of solid reaction products. It is substantially lower than the activation energy threshold for surface chemical reaction control (>40 kJ·mol^{-1}). To further validate this interpretation, the obtained E_a was compared with literature data for nickel leaching from analogous low-grade silicate and technogenic feedstocks under various acid systems. For diffusion-controlled regimes, the following values have been reported: 11.57 kJ·mol^{-1} for sulphuric acid leaching of serpentine [Wu et al. 2022], 12.9 kJ·mol^{-1} for sulphuric acid leaching of oxidised nickel ore with NaF additive Klyushnikov 2018], and 16.6 kJ·mol^{-1} for nickel extraction from spent NiO/Al_2O_3 catalyst in H_2SO_4 medium [Mulak et al., 2005]. In contrast, chemically controlled processes exhibit considerably higher activation energies, such as 76.07 kJ·mol^{-1} and 74.52 kJ·mol^{-1} reported for hydrochloric acid leaching of lateritic nickel ores [Shayakhmetova et al. 2025; Ağaçayak et al. 2011], where the surface chemical reaction is rate-determining. The close agreement of the present E_a value (18.4 kJ·mol^{-1}) with those characteristic of internal diffusion strongly supports the conclusion that the nitric acid leaching of the magnetic fraction proceeds under mass-transfer control. The slight elevation of this value relative to that for pure serpentine (11.57 kJ·mol^{-1}) can be rationalised by the mineralogical complexity of the magnetic fraction. As evidenced by X-ray diffraction, this fraction contains compact ferrite phases - specifically nickel ferrite ($NiFe_2O_4$) and magnesioferrite ($Mg_{0.04}Fe_{2.96}O_4$). These spinel-type structures are less permeable than serpentine minerals and generate a denser product layer during acid attack, thereby increasing the diffusion resistance. Nevertheless, the E_a remains well within the diffusion-controlled interval.

Consequently, the overall rate of nickel extraction from the magnetic fraction of asbestos waste by nitric acid is governed by the mass transfer of ions through the evolving porous structure of the undissolved residue, rather than by the kinetics of the chemical reaction at the phase interface. The pre-exponential factor, calculated from the y-intercept of the Arrhenius plot as $A = 2.84 \cdot 10^2$ min^{-1}, reflects the collision frequency of the reacting species and is consistent with the moderate viscosity of aqueous nitric acid solutions under the studied temperature range.

Finally, thermodynamic analysis confirms that raising the temperature from 25 °C to 85 °C results in a 4.7-fold increase in the leaching rate constant. This quantitatively explains the observed enhancement in nickel extraction efficiency from 42.3% to 89.7% (all other conditions

being equal), underscoring the decisive role of temperature in overcoming diffusion barriers in this heterogeneous system.

CONCLUSION

The conducted research confirms the high efficiency of using magnetic separation as a method for the pre-concentration of nickel-containing phases, which significantly optimizes the subsequent nitric acid leaching process. It was established that the temperature factor is the determining parameter for intensifying metal extraction, providing an increase from 42.3% to 74.1% when the temperature is raised to 85 °C. A comprehensive kinetic analysis revealed that the process is most adequately described by the Drozdov - Rotinyan equation, which accounts for the formation of a solid reaction product layer and the inhibitory effect caused by the blocking of active sites. The calculated apparent activation energy of 18.4 kJ/mol serves as fundamental evidence that the overall reaction rate is limited by internal diffusion resistance. Given the high iron oxide content in the magnetic fraction, the rate-limiting stage is the mass transfer of ions through the developing structure of the undissolved residue, which prevents the reagent from freely accessing the reaction front. Thus, to achieve maximum technological performance, it is necessary to maintain intensive hydrodynamic regimes to reduce diffusion barriers. The proposed approach to processing the magnetic fraction opens new perspectives for reclassifying asbestos tailings as valuable secondary resources, ensuring the production of high-demand nickel compounds while simultaneously reducing the environmental impact on the region.

CONFLICT OF INTEREST: The authors declare that they have no conflicts of interest.

FUNDING: This research was funded by the Science Committee of the Ministry of Science and Higher Education of the Republic of Kazakhstan (grant No. AP26100359).

INSTITUTIONAL REVIEW BOARD STATEMENT: Not applicable.

INFORMED CONSENT STATEMENT: Not applicable.

DATA AVAILABILITY STATEMENT: The data supporting the findings of this technical study are available from the corresponding author upon reasonable request.

ACKNOWLEDGEMENTS: The authors express their gratitude to colleagues for methodological support and helpful discussions, as well as to anonymous reviewers for valuable comments that helped improve the quality of the article.

STATEMENT ON THE USE OF ARTIFICIAL INTELLIGENCE TECHNOLOGIES: The authors of the scientific article declare that they did not use artificial intelligence (AI) tools at any stage of the preparation of their work, including text writing, editing, fact-checking, or data analysis.

REFERENCES

Abdirashit, A., Kelamanov, B., Sariyev, O., Yessengaliyev, D., Abilberikova, A., Zhuniskaliyev, T., Kuatbay, Ye., Naurazbayev, M., & Nazargali, A. (2025). Study of nickel–chromium-containing ferroalloy production. Processes, 13(4), 1258. https://doi.org/10.3390/pr13041258

Agacayak, T., Zedef, V., & Aydogan, S. (2011). Leaching of lateritic nickel ores of Karacam (Eskisehir-Turkey) with hydrochloric acid. International Multidisciplinary Scientific GeoConference: SGEM, 1, 1155.

Arynov, K., Auyeshov, A., Yeskibayeva, S., Auyeshov, D., & Beisbekova, R. (2017). Study of chemical and mineral compositions of chrysotile asbestos production dusty wastes. Industrial Technology and Engineering, (2), 28–34. https://www.elibrary.ru/item.asp?id=38572717

Baigenzhenov, O. S., Chepushtanova, T. A., Altmyshbayeva, A. Z., Temirgali, I. A., Maldybayev, G., Sharipov, R. H., Altaibayev, B. T., & Dagubayeva, A. T. (2024). Investigation of thermodynamic and kinetic regularities of asbestos waste leaching processes. Results in Engineering, 21, 102000. https://doi.org/10.1016/j.rineng.2024.102000

Baigenzhenov, O.S., Kozlov, V.A., Luganov, V.A., Mishra, B., Shayahmetova, R.A., & Aimbetova, I. O. (2015). Complex processing of wastes generated in chrysotile asbestos production. Mineral Processing and Extractive Metallurgy Review, 36(4), 242–248. https://doi.org/10.1080/08827508.2014.955610

Chen, T.T., Dutrizac, J.E., & White, C. (2000). Serpentine ore microtextures occurring in the Magnola magnesium process. JOM, 52(4), 20–22. https://doi.org/10.1007/s11837-000-0125-x

Doménech-Carbó, A. (2024). Exploring nucleation modeling of the voltammetry of solid-to-solid-state redox processes with phase changes. Journal of Solid State Electrochemistry, 28(5), 1497–1507. https://doi.org/10.1007/s10008-023-05572-0

Fournier, J., Régnier, E., Faure, F., Le Goff, X., Brau, H. P., Brackx, E., & Pinet, O. (2018). Modeling of dissolution kinetics of rare earth crystals in a borosilicate glass melt. Journal of Non-Crystalline Solids, 481, 248–253. https://doi.org/10.1016/j.jnoncrysol.2017.10.042

Ivanov, N. S., Kholkin, O. S., Abilmagzhanov, A. Z., Adelbayev, I. E., Oparin, S. K., Ivanova, N., & Kudryashov, V. (2025). Nitric acid leaching for magnesium extraction from asbestos ore waste: From DoE to predictive modeling and cost-efficient optimization. Molecules, 30(22), 4396. https://doi.org/10.3390/molecules30224396

Kelamanov, B., Samuratov, Y., Akuov, A., Abdirashit, A., Burumbayev, A., & Orynbassar, R. (2021). Research possibility of involvement Kazakhstani nickel ore in the metallurgical treatment. Metalurgija, 60(3-4), 313–316. https://hrcak.srce.hr/index.php/en/clanak/372261

Kenzhaliyev, B., Ultarakova, A., Lokhova, N., Mukangaliyeva, A., & Kassymzhanov, K. (2025). Optimized hydrometallurgical extraction of molybdenum via mechanoactivation and nitric–sulfuric leaching. Processes, 13(5), 1486. https://doi.org/10.3390/pr13051486

Klyushnikov, A. M. (2018). Sulphuric-acid leaching of ural oxidized nickel ore with sodium sulfite and fluoride additives. Journal of Mining Science, 54(1), 141-146. https://doi.org/10.1134/S1062739118013450

Kovalevskiy, E. V., Sharshenova, A. A., Tshomariia, I. M., & Zh, O. Y. (2024). Evaluation of potential risks of air pollution by asbestos fibres. Evaluation, 2024(4). https://dx.doi.org/10.51350/zdravkg2024.4.12.15.116.125

Mulak, W., Miazga, B., & Szymczycha, A. (2005). Kinetics of nickel leaching from spent catalyst in sulphuric acid solution. International Journal of Mineral Processing, 77(4), 231-235. https://doi.org/10.1016/j.minpro.2005.06.005

Petrovski, A., Načevski, G., Dimitrov, A. T., & Paunović, P. (2019). Kinetic models of nickel laterite ore leaching process. Machines. Technologies. Materials., 13(11), 487–490.

Shayakhmetova, R. A., Mukhametzhanova, A. A., Akbayeva, D. N., Terlikbaeva, A. Z., Osipov, P. A., Alimzhanova, A. M., & Zharmenov, A. A. (2024). Magnesium and silicon recovery from chrysotile asbestos waste of the deposit Zhitikara, Kazakhstan. Scientific Reports, 14(1), 31866. https://doi.org/10.1038/s41598-024-83239-0

Shayakhmetova, R., Mukhametzhanova, A., Osipov, P., Kali, A., Kuandykova, A., & Rakhym, A. (2025). Mechanism, kinetics and thermodynamics of nickel, iron, and magnesium hydrochloric acid leaching from laterite ore. Scientific Reports, 15(1), 41342. https://doi.org/10.1038/s41598-025-25276-x

Shevko, V.M., Akylbekov, Y.Y., Karataeva, G.Y., & Badikova, A.D. (2022). Recycling of chrysotile-asbestos production waste. Metallurgical Research & Technology, 119(4), 410. https://doi.org/10.1051/metal/2022050

Tauakelov, C.A., Rakhimbayev, B.S., Yskak, A., Valiev, K.K., Tastanov, Y.A., Ibrayev, M.K., Bulayev, A., Daribayeva, S., Kazbekova, K., & Joldassov, A. A. (2025). Treatment of refractory oxidized nickel ores (ONOs) from the Shevchenkovskoye ore deposit. Metals, 15(8), 876. https://doi.org/10.3390/met15080876

Wang, Y., Li, K., Sun, H., Yu, H., Jiang, B., Liu, J., & Zhang, Z. (2025). Recovery of magnesium from iron ore tailings: Acid leaching kinetics and CO_2 mineralization. Physica Scripta, 100(8), 0859a8. https://doi.org/10.1088/1402-4896/adfd31

Wu, L. L., Yang, X. Y., Xu, H., Zhong, Z. J., & Wang, X. D. (2022). Kinetic study of high-pressure acid leaching of Mg and Ni from serpentine. Journal of Central South University, 29(2), 410-419. https://doi.org/10.1007/s11771-022-4912-1

Yessengaziyev, A., Toishybek, A., Mukangaliyeva, A., Altaibayev, B., Smailov, K., Yersaiynova, A., & Abdyldayev, N. (2025). Kinetics of acid leaching of niobium from man-made raw materials of titanium magnesium production: Experimental research and modelling. Processes, 13(6), 1924. https://doi.org/10.3390/pr13061924

Zmpitas, J., & Gross, J. (2021). Modified Stokes–Einstein equation for molecular self-diffusion based on entropy scaling. Industrial & Engineering Chemistry Research, 60(11), 4453–4459. https://doi.org/10.1021/acs.iecr.0c06090

Zoraga, M., Ilhan, S., & Kalpakli, A. O. (2020). Leaching kinetics of electric arc furnace dust in nitric acid solutions. International Journal of Chemical Kinetics, 52(12), 933–942. https://doi.org/10.1002/kin.21411

Information about authors

Baigenzhenov Omirserik – PhD, Professor, Satbayev University, Almaty, Kazakhstan.
e-mail: o.baigenzhenov@satbayev.university
ORCID: https://orcid.org/0000-0001-5803-7680

Assel Dagubayeva – PhD student, Kazakh-British Technical University, Almaty, Kazakhstan
e-mail: a.dagubayeva@kbtu.kz
ORCID: https://orcid.org/0000-0002-2675-0577

Galymzhan Maldybayev – Associate Professor, Kazakh-British Technical University, Almaty, Kazakhstan
e-mail: g.maldybayev@kbtu.kz
ORCID: https://orcid.org/0000-0003-3592-5671

Rustam Sharipov – Head of Laboratory, Kazakh-British Technical University, Almaty, Kazakhstan.
e-mail: r.sharipov@kbtu.kz
ORCID: https://orcid.org/0000-0003-1670-9914

Aliya Margulanovna Alimzhanova – PhD, Head of the Laboratory of «Special Methods of Raw Material Beneficiation», National Center for Complex Processing of Mineral Raw Materials of the Republic of Kazakhstan, Almaty, Kazakhstan.
e-mail: aliyuchca@gmail.com
ORCID: https://orcid.org/0000-0001-6098-7626